Progress In Electromagnetics Research M, Vol. 93, 99–108, 2020

Design of a Beam Switchtable Superdirective Dipole for IoT Gateway

Sana Souai[1, *], Aliou Diallo[1], Jean Marc Ribero[1], and Taouifik Aguili[2]

Abstract—In this paper, a switchable beam and super-directive Electrically Small Antenna (ESA) dipole deployed at an IoT network gateway at 868 MHz is presented. It consists of one fed dipole and one loaded parasitic dipole. The nature and value of the load are obtained using the Uzkov equations, allowing determining current weighting coefficients in the case of two separately fed antennas, in order to maximize the gain and the directivity in a given direction. Reconfigurability in two directions is achieved using a pair of anti-parallel PIN diodes to steer the beam to the desired direction. The array final dimensions are $109 \times 43\,\text{mm}^2$ ($0.3\lambda \times 0.1\lambda$) generating a high directivity of 6.8 dBi in simulation and 6.7 dBi in measurement at 868 MHz for each beam in the azimuth plane.

1. INTRODUCTION

Nowadays, the modern world has become connected. The size of mobile terminals and the multiplication of communicating objects for wireless communications generate a need for Electrically Small Antennas (ESA) with better performance. The limits of ESA in terms of quality factor, bandwidth, gain, and directivity have been widely studied in the literature [1]. In 1958, Harrington [2] established a limit of maximum directivity D that a single ESA can reach: $D_{\max} = (ka)^2 + 2(ka)$, where Ka is the antenna electrical size.

Several directivity enhancement techniques have been studied in the literature with the introduction of super directivity. It is in this sense that Uzkov has demonstrated that the directivity to the main end-fire direction of N isotropic radiating elements placed close to each other (inter-element distance near zero) can reach N^2 [3]. The super-directivity method has been presented in several articles. It consists of feeding one antenna and loading the second one (the parasitic element) with a load calculated from the weighting coefficients and Z parameters [4, 5].

Pigeon et al. presented a planar array antenna [6], and Haskou and Sharaiha integrated an array of two CPW-fed spiral antennas in a Printed Circuit Board (PCB) and achieved an important gain, but it was low in efficiency [7]. Haskou et al. studied an array of two superdirective ESAs where the unit element was a printed half-loop antenna integrated on PCB [8].

Reconfigurable antennas can change their frequency, radiation pattern, or the polarization to increase antennas functionality. The concept of beam steering using parasitic radiators in order to alter the antenna radiation patterns without a significant change in other characteristics especially impedance matching by electronically controlling tunable loads was introduced by Harrington [9] in the 1970's. Then, Milne replaced tunable loads with a simple On/Off RF switch (using PIN diodes) [10] which facilitated beam steering by controlling the phases of the currents in the passive radiators to estimate the value of the capacitances or inductances required to focus the beam on a particular direction.

In [11], a novel radiation-pattern-reconfigurable antenna that could operate in four directions without any antenna servo system was achieved by changing the wave director and wave reflector

Received 2 April 2020, Accepted 27 May 2020, Scheduled 10 June 2020

* Corresponding author: Sana Souai (Sana.SOUAI@univ-cotedazur.fr).

[1] LEAT: University of Nice Cote d'Azur, France. [2] Sys'Com: University of Tunis ELMANAR, National Engineers School of Tunis, Tunisia.

via appropriate pin diodes. Dhissou et al. resorted to this method to present a directive four switchable beam antenna at 2.45 GHz for WIFI applications [12].

The solution proposed in this paper is compared with similar research works in the literature [7–12] and presented in Table 1.

Table 1. Comparison with existing studies on superdirective and reconfigurable antenna.

Author	Structure of the antenna	Resonant Frquency (GHz)	Maximum total directivity (dBi)/ gain (dBi)	reconfigurability method	beam directions in degree
[7]	2 small printed CPW-fed spiral antenna	0.830	7.2 (Directivity)	None	180 (Azimuth plane)
[8]	Two miniaturized printed half-loop antenna on PCB	0.905	7.2 (Directivity)	None	−90 (Azimuth plane)
[9]	Seven-element circulararray of reactively loaded dipoles	None	6.76 (Gain)	Multiport	0, 10, 20, 30 (Elevation plane)
[10]	A driven monopole with two concentric rings of 8 parasitic elements	1.5	None	Pin diodes	30, 40 (Elevation plane)
[11]	Dipole +2 directors +2 reflectors	2.5	5.08 (Gain)	Four pin diodes	0, 90, 180, −90 (Azimuth plane)
[12]	Four monopoles (2 Monopoles +2 loaded parasitic elements)	2.45	5.2 (Gain)	Switching reflectors or directors +PIN diode	0, 90, 180, 270 (Azimuth plane)
Our work	Two meandered folded dipole (one fed dipole and one parasitic dipole)	0.868	6.8 (Directivity)	two PIN diode	0, 180 (Azimuth plane)

The loaded parasitic array antennas appear through the state of the art as a promising solution to create directional beam and avoid mutual coupling that can be produced between two fed antennas which reduce the efficiency of the system. This principle of super-directivity with reconfigurable beam can be interesting for Internet of Things (IoT) gateways for reducing energy consumption at the connected object and for improving the robustness of communication.

In this paper, our interest focuses on the capability of an Electrically Small Antennas for IoT gateway to be:

(i) Super-directive without increasing impedance mismatch causing antenna's efficiency degradation.

(ii) Reconfigurable beam steering to generate two different beam patterns.

This work is organized as follows. First, we propose the establishment of an array dipole antenna using the meander technique and discuss the use of a stub to correct antenna impedance mismatch. The optimization process to enhance the antenna directivity has also been presented in Section 2.2. Next, we study electronically reconfigurable beam steering of the proposed antenna using embedded RF PIN switches. In the last part, we highlight the obtained simulated and measured results of the super directive and reconfigurable beam steering antenna.

2. DESIGN METHODOLOGY

2.1. Geometry of the Proposed Antenna

In order to develop and design an Electrically Small Antenna for IoT gateway application, the proposed antenna consists of two meandered dipoles (periodically folded); each dipole has a length of 0.3λ, and the inter-element spacing is set to 0.09λ, where λ represents the wavelength at 868 MHz, and the final optimized dimensions of the simulated antenna structure are: $L = 103$, $d = 30$, and $W = 43$.

The proposed antenna has 2 electrically small antennas dipoles. The substrate used to fabricate the antenna is FR4 having dielectric constant of 4.4 ($\tan\delta = 0.02$) and thickness of 0.8 mm as shown in Fig. 1.

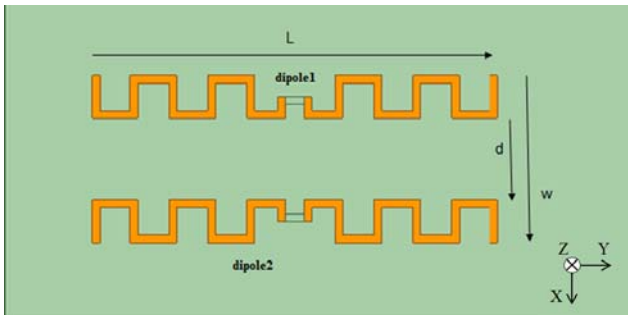

Figure 1. Geometry of the proposed array antenna.

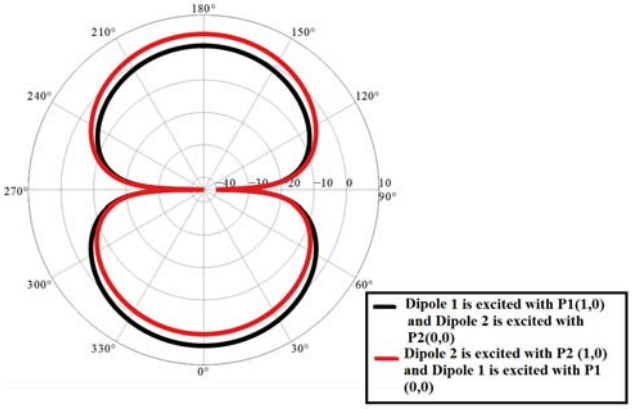

Figure 2. Simulated 2D total directivity of the driven array at 868 MHz in the azimuth plane when the two dipoles are alternately excited.

Figure 1 shows the proposed array antenna where both dipoles are alternately excited. ANSYS HFSS software is used to provide simulations results. Fig. 2 illustrates the radiation pattern in azimuth plane ($\theta = 90°$). A simulated total directivity of almost 4 dBi is obtained in the direction ($\theta = 90°, \phi = 0°$) when dipole 1 is excited and in the direction ($\theta = 90°, \phi = 180°$) when dipole 2 is excited which is less than Harrington's normal directivity limit of an antenna with the same dimensions $ka = 1.8$ (4.8 dBi).

2.2. Directivity Enhancement

In order to improve the directivity of the proposed antenna, dipole 1 is maintained as a driven element and dipole 2 as a parasitic element loaded by Z_L to obtain a super-directive functionality and to achieve a minimum directivity of 6 dBi (N^2) as announced by Uzkov.

The antenna array is simulated via the ANSYS HFSS simulation software, and the first element is excited with an amplitude of 1 and a phase of 0° while the excitation of the second element will be adjusted corresponding to a variation of the power ratio P1/P2 where P1 and P2 are respectively the power of dipole 1 and dipole 2.

The radiated electrical fields obtained from an electromagnetic simuflator are integrated in equations by Uzkov [3] in order to calculate the required current excitation coefficients that improve the directivity in a given direction at 868 MHz. The current excitation coefficients that maximize the directivity in the direction (θ_0, ϕ_0) are given by:

$$a_{02} = [H_{12}^*]^{-1} e^{-jkr_0r_2} f_1^*(\theta_0, \phi_0) f_2(\theta_0, \phi_0). \quad (1)$$

a_{02} is the current ratio between the feeding ports and can be expressed according to the power

ratio P1/P2 and Z-parameters. H_{12} is obtained from the Uzkov equation, and it is revealed by:

$$H_{12} = \frac{1}{4\pi} \sum_{\theta=0}^{\theta=2\pi} \sum_{\phi=0}^{\phi=\pi} f_1(\theta,\phi) f_2^*(\theta,\phi) e^{jkr(r_2-r_1)} \sin(\theta)\Delta(\theta)\Delta(\phi). \quad (2)$$

r is the unit vector in the far-field direction (θ_0, ϕ_0); $r_2 - r_1$ is the distance between the feeding port positions P2 and P1 of the antennas.

$k = \frac{w}{c}$ is the wave number; f_1 and f_2 are the radiated electrical fields in the far field direction (θ, ϕ).

$$f_1 = E_{\theta 1} + E_{\phi 1}. \quad (3)$$

$$f_1 = E_{\theta 2} + E_{\phi 2}. \quad (4)$$

$\Delta(\theta) = \frac{2\pi}{N_\theta}$ and $\Delta(\phi) = \frac{2\pi}{N_\phi}$ are the far-field sampling steps in the spherical angles (θ, ϕ); N_θ and N_ϕ are the number of samples.

A simulated directivity of 7 dBi is achieved in the direction $(\theta = 90°, \phi = 180°)$ when exciting each element respectively by P1 (1 W, 0° and P2 (0.87 W, 65°) (Fig. 3). The second dipole is then transformed into a parasitic element, and its excitation is transformed into a charge Z_L using Equations (5) and (6).

$$Z_{\text{active}}(2) = \frac{V2}{I2} = Z_{22} + Z_{21} * \frac{I1}{I2}. \quad (5)$$

$$Z_L(2) = -Z_{\text{active}}(2) \quad (6)$$

where $V2$ and $I2$ define respectively the input voltage and current of the parasitic antenna.

The parameters Z_{ii} are derived from impedance matrix $[Z]$ which can be used with the current excitation to calculate the power excitation coefficients necessary to enhance the directivity of the array antenna.

The charge needed to optimize the directivity of the proposed array antenna in the azimuth plane, evaluated at 868 MHz, corresponds to an inductor $L = 33$ nH.

This load (an inductor) was performed on the second dipole, and a good directivity of 7 dBi (Fig. 3) was achieved, but an impedance mismatch ($|S_{11}| = -3$ dB at 868 MHz) was faced in the European IoT band [863–870 MHz] as shown in Fig. 4. This phenomenon can greatly reduce the realized gain (which is the actual gain taken into account in the transmission chain) by 50% without even taking into account the radiated efficiency.

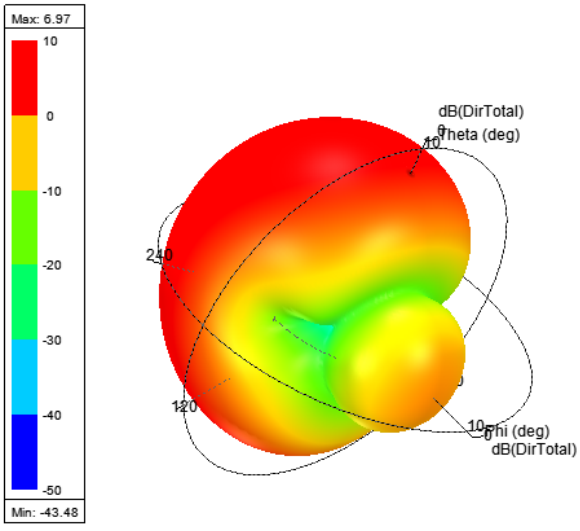

Figure 3. Simulated 3D radiation pattern at 868 MHz when dipole 1 is excited by P1 (1 W, 0°) and dipole 2 by P2 (0.85 W, 65°).

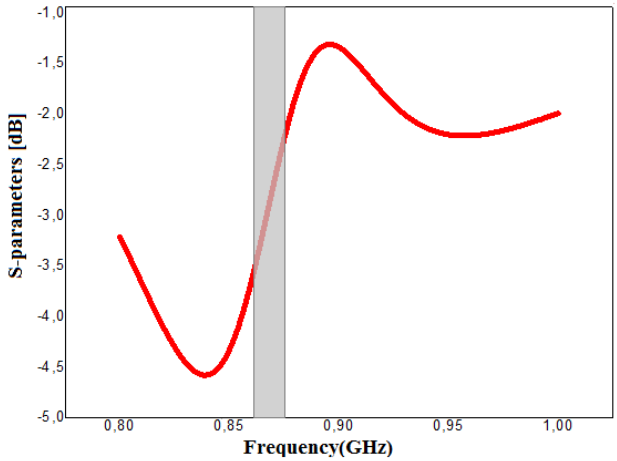

Figure 4. Simulated reflection coefficient of the system with the load ZL.

There are several techniques that can be applied to correct antenna impedance mismatch. In this paper, we propose to use the stub tuning method; the stub operates as a parallel inductor to the RLC circuit.

The length, width, and position of the stub have been adjusted to suitably match the antenna impedance at the operating frequency 868 MHz. It was connected in parallel to each dipole and placed respectively at 3 mm from the excitation (fed element) and the load (parasitic element). The optimum stub length and width are respectively $ls = 22$ mm and $ws = 1$ mm as illustrated in Fig. 5.

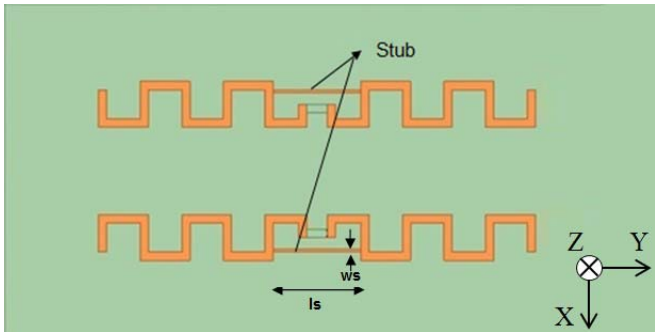

Figure 5. Geometry of the array antenna with two stubs.

A reflection coefficient equal to −25 dB is obtained at 868 MHz as shown in Fig. 6 which confirms that attaching the stub to each meandered dipole can improve the impedance matching of the proposed antenna in the operating band [863–870 MHz]. A simulated radiation efficiency around 72% of the super directive antenna is obtained at 868 MHz as shown in Fig. 7.

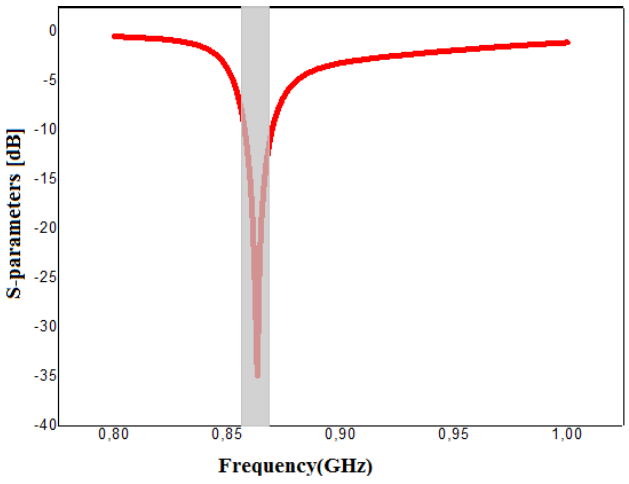

Figure 6. Simulated reflection coefficient of the proposed antenna.

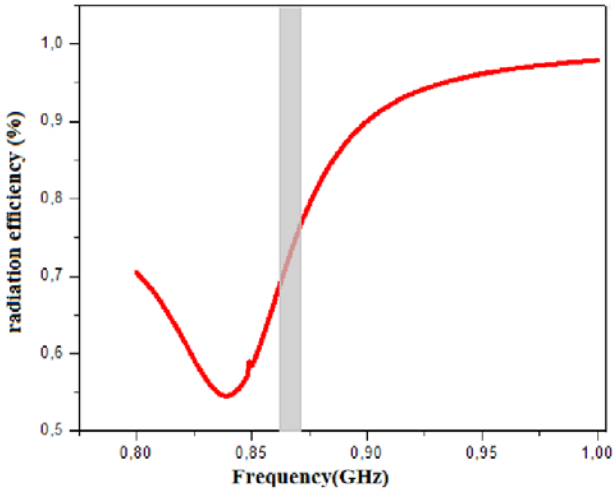

Figure 7. Simulated radiation efficiency of the proposed structure.

In the next section, we will discuss the capacity of the proposed antenna to perform the beam steering using an active component.

3. RECONFIGURABLE ANTENNA DESIGN

The main idea from reconfiguring the array antenna is to control the array field pattern to change the maximum beam shape and alter the side lobe levels.

To achieve the beam-reconfigurability, the proposed structure is the same as the one described in Section 1: An array of two electrically small antennas where the unit element is a meandered dipole, one driven element, and one parasitic element where two loads in series with a pair of anti-parallel pin diode are placed at the gap and two metallic vias connecting the front and back layer of the substrate to feed the pin diode.

PIN diodes operate as a current controlled resistor at radio frequencies and microwave circuits; they have been used for RF switching of reconfigurable antennas.

In this work, a BAR64-04W PIN diode from Infineon Technologies is used; the equivalent circuit of the PIN diode in the ON and OFF states is shown in Fig. 8.

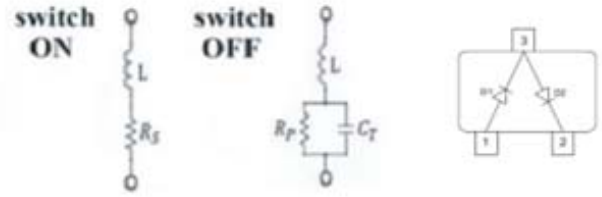

Figure 8. Equivalent circuit of the BAR64-04W PIN diode.

Both the ON and OFF states have a package inductance L. The equivalent circuit in the ON state (forward biased) has a low resistance Rs which contributes to the insertion loss. The equivalent circuit for OFF state (zero or reverse biased) has the parallel combination of the reverse bias resistance Rp and the total capacitance CT which contributes to isolation.

The parameter values of the equivalent circuit model are given in Table 2 corresponding to the datasheet of the PIN diode used.

Table 2. Parameter values of the PIN diode equivalent circuit at 1 GHz.

Diode	State	Parameters			
		$Rp\,(\Omega)$	$Rs\,(\Omega)$	L (nH)	CT (pF)
Pin	on		1.5	1.4	
	off	3500		1.4	0.23

The proposed reconfigurable antenna design and the equivalent circuit modeled in ANSYS HFSS software of the BAR64-04W PIN diode in the ON and OFF states are illustrated in Fig. 9.

The biasing network was modeled as a 220 nH inductor and a 50 Ω resistor in series as RF isolators, a capacitor of 220 pF as DC blocks. The PIN diodes are biased by applying a voltage of 3.3 V or −3.3 V. By controlling the biasing of the PIN diodes, the antenna is made reconfigurable.

Two possible configurations of the antennas are as follows:

(i) If the DC voltage across the PIN diode is +3.3 V, D1 is turned ON and D2 turned OFF: the parasitic element is loaded by load 1.

(ii) If the DC voltage across the PIN diode is −3.3 V, D1 is turned OFF and D2 turned ON: the parasitic element is loaded by load 2.

The optimization process described in Section 2.2 was used to calculate the required current excitation coefficients that maximize the directivity and reconfigure the main beam of the radiation pattern into two different desired directions with respect to the impedance matching. The amplitude and phase weighting to apply to the parasitic antenna have been calculated using Uzkov formula.

The nature of the required loads to maximize the directivity and achieve the two beam steering directions of the azimuth plane: $(\theta = 90°, \phi = 180°)$ and $(\theta = 90°, \phi = 0°)$ are respectively a resistor of 68 Ω in series with an inductor of 33 nH and a negative resistor of −5 Ω in series with a capacitor of 5.6 pF. The loading of the proposed antenna by the previously calculated loads makes it possible to find the expected behavior of beam steering and super directivity. The maximum simulated directivity values in the two steered beam directions are all about 6.8 dBi as shown in Fig. 10.

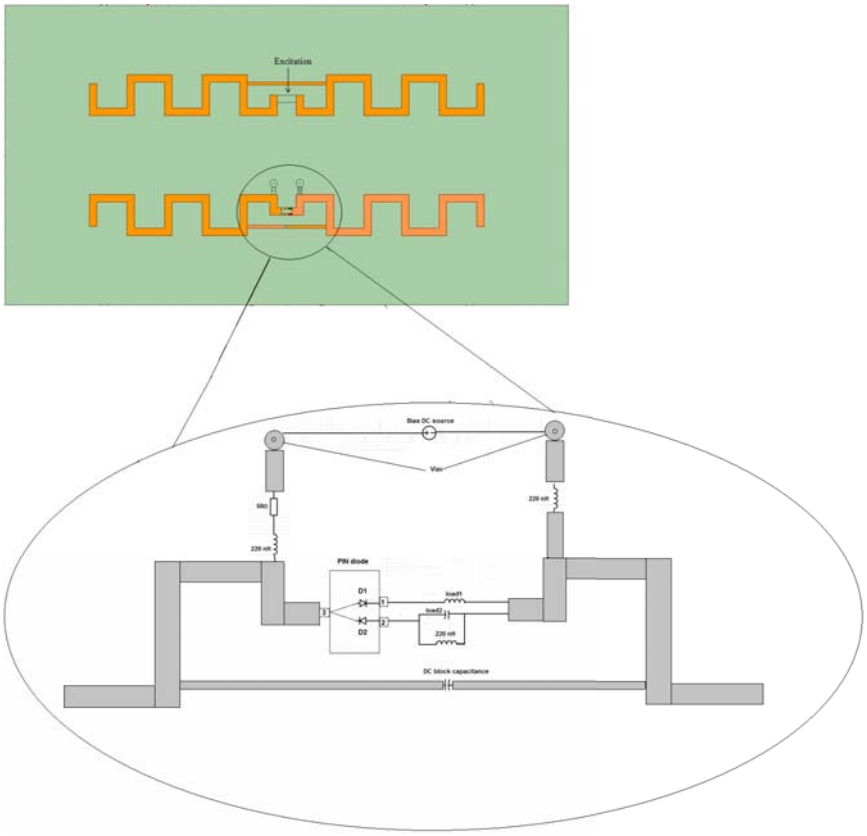

Figure 9. Geometry of the proposed reconfigurable antenna.

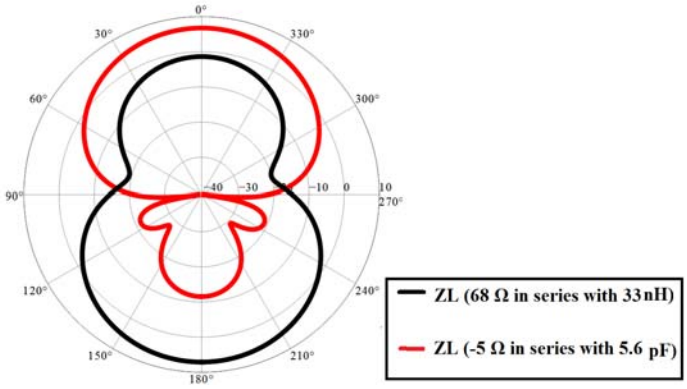

Figure 10. Simulated 2D total directivity in the azimuth plane at 868 MHz of the two-element array.

In this paper, neither the resistive negative part nor the positive part of the synthesized impedances is included in the fabrication process. Fig. 11 compares the directivity of the antenna loaded only by an inductive load of 33 nH and the directivity when the antenna is loaded by the inductive load in series with a resistor of 68 Ω.

As shown in Fig. 11, we observe that the loading of the parasitic antenna with only an inductor gives better side lobes.

Figure 12 compares the directivity of the proposed array antenna loaded only by a capacitive load of 5.6 pF and the directivity of the active network loaded by the synthesized loads from the weighting coefficients (capacitor of 5.6 pF in series with negative resistor of −5 Ω). A simulated total directivity of

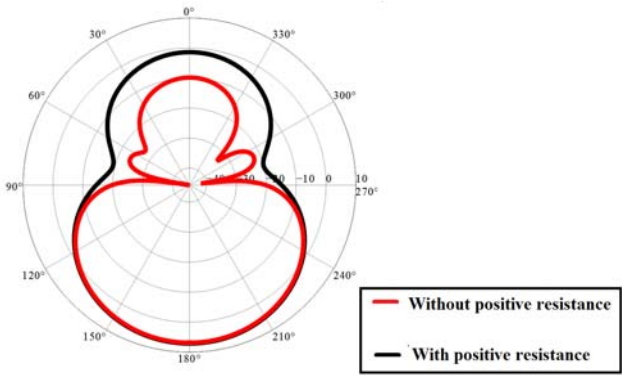

Figure 11. Two-element array's simulated 2D total directivity in the azimuth plane at 868 MHz with $L = 33\,\text{nH}$ in series with and without positive resistor $68\,\Omega$.

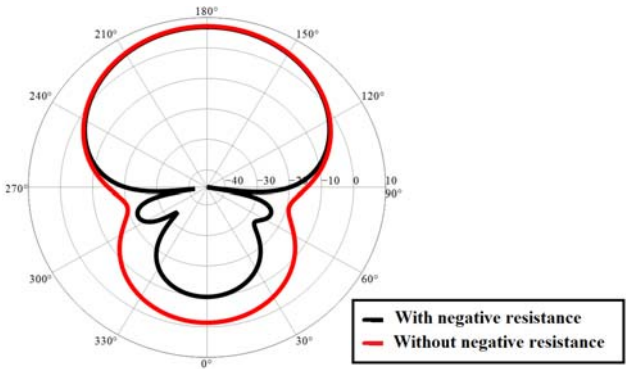

Figure 12. Two-element array's simulated 2D total directivity in the azimuth plane at 868 MHz with $C = 5.6\,\text{pF}$ in series with and without negative resistor $-5\,\Omega$.

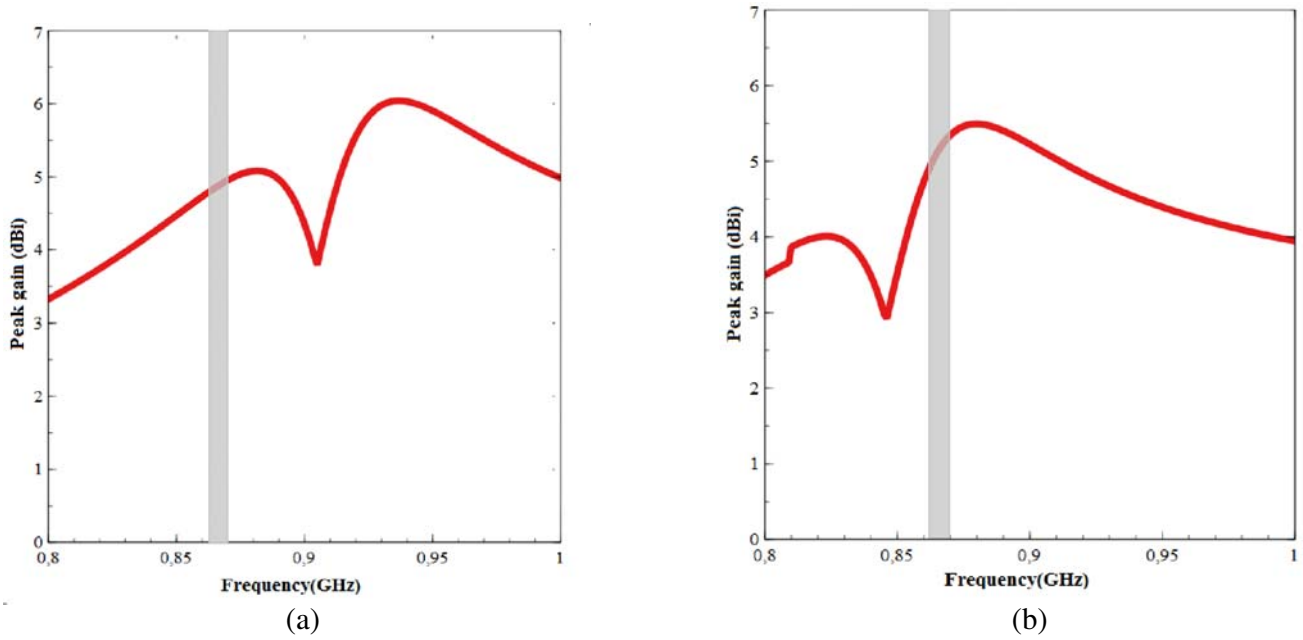

Figure 13. Simulated peak gain of the two-element array: (a) for $Z_L = 5.6\,\text{pF}$, (b) for $Z_L = 33\,\text{nH}$.

6.3 dBi is obtained when the parasitic antenna is loaded by only a capacitor of 5.6 pF; we can see that the side lobe level (SLL) has increased from −11 dBi to −0.56 dBi. This study shows that the negative resistance in addition of increasing the impedance matching bandwidth [13] maintains low side lobes.

So, instead of discrete components, an NIC (Negative Impedance Converter) circuit could be used for Z_L, to reduce the back lobes.

The peak gain plot versus frequency is shown in Fig. 13. The obtained peak gain at the operating frequency is 5.26 dBi when the parasitic antenna is loaded by an inductive load of 33 nH (Fig. 13(b)) and almost 5 dBi when the parasitic antenna is loaded by a capacitive load of 5.6 pF (Fig. 13(a)).

A prototype of the proposed array antenna was realized on a 0.8 mm thick FR4 substrate of relative permittivity $\epsilon_r = 4.4$. A photo of the prototype is shown in Fig. 14. The reflection coefficient versus frequency results from the measurement of the proposed antenna are shown in Fig. 15. At the center frequency 868 MHz, the measured reflection coefficient is −17 dB. A frequency shift less than 1% and quite different return loss results are observed between the simulation and measurement, which can be due to the variation of the properties of commercial HFSS substrate and the SMA connector effect used

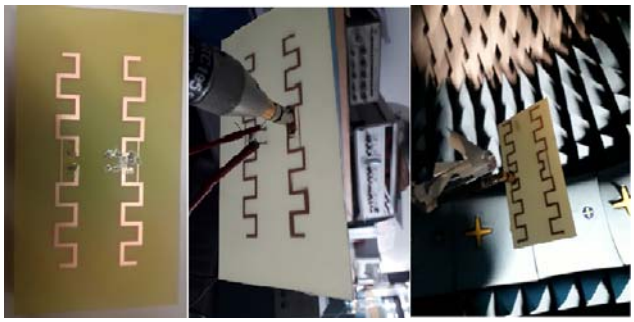

Figure 14. Photograph of the prototype of super directive reconfigurable antenna.

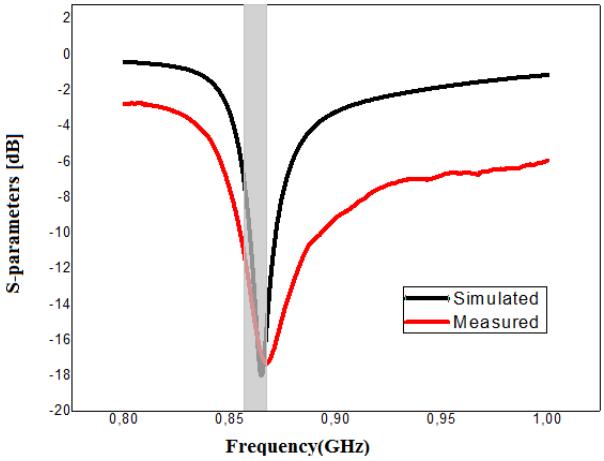

Figure 15. Simulated and measured return loss for $Z_L = 5.6\,\text{pF}$.

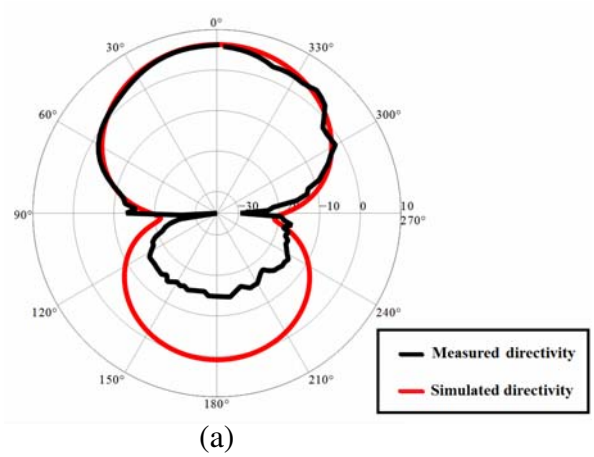

(a)

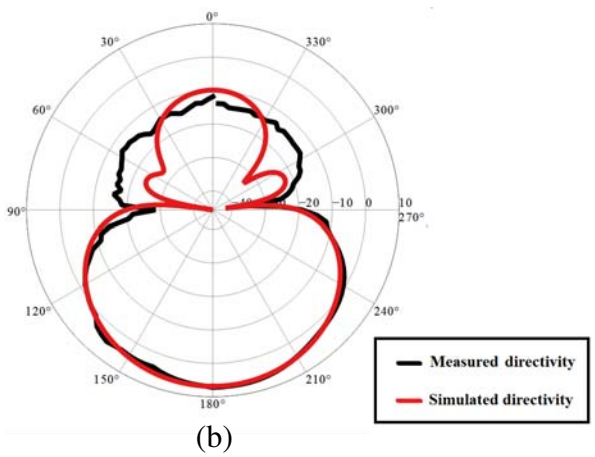

(b)

Figure 16. Measured and simulated 2D total directivity at 868 MHz of the two-element array: (a) Maximum directivity achieved for $Z_L = 5.6\,\text{pF}$, (b) maximum directivity achieved for $Z_L = 33\,\text{nH}$.

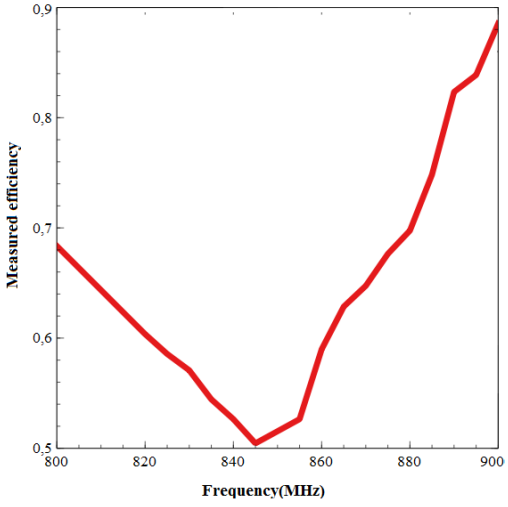

Figure 17. Measured total efficiency for $Z_L = 5.6\,\text{pF}$.

in the measuring system.

The antenna 3D far-field radiation pattern and efficiency are measured in the laboratory using the SATIMO near-field measurement system.

Figure 16 illustrates the measured radiation pattern at 868 MHz. We have found that the total directivity is close to 6.7 dBi in the desired direction, proving a good agreement between the simulated and measured results in the two directions of the azimuth plane.

In Fig. 17, we show the measured total efficiency of the array antenna. For $Z_L = 5.6$ pF, we obtain a total efficiency higher than 60% in the European IoT band.

4. CONCLUSION

This article proposes the implementation of a two-element super directive Electrically Small Antenna (ESA) array that can steer the beam in two directions in the azimuth plane by employing one embedded RF PIN diode for IoT gateway. One of the dipoles is transformed into a loaded parasitic element calculated from the weighting coefficients and Z parameters. The achieved results show the maximum total directivity of 6.8 dBi in simulation and 6.7 dBi measured at 868 MHz in the two states of switching configuration. Measurement results on the array input parameters are in full match with simulated ones. This work could be extended by using another pair of similar dipoles placed perpendicularly to cover the 4 directions (0°, 90°, 180°, −90°) in the azimuth plane, as well as NIC circuits as charge to reduce the back lobes very strongly.

REFERENCES

1. Wheeler, H. A., "Fundamental limitations of small antennas," *Proc. IRE*, Vol. 35, No. 12, 1479–1484, Dec. 1947.
2. Harrington, R. F., "On the gain and beamwidth of directional antennas," *IRE Transactions on Antennas and Propagation*, 219–225, Jul. 1958.
3. Uzkov, I., "An approach to the problem of optimum directive antennae design," *Comptes rendues (Do lady) de l'académie des sciences de l'URSS*, Vol. 53, No. 1, 35–38, 1946.
4. O'Donnell, T. H. and A. D. Yaghjian, "Electrically small superdirective arrays using parasitic element," *IEEE Antennas and Propagation Society International Symposium*, 3111–3114, Jul. 2006.
5. Boyle, K., "Radiation patterns and correlation of closely spaced linear antennas," *IEEE Trans. Antennas Propag.*, Vol. 50, No. 8, 1162–1165, Aug. 2002.
6. Pigeon, M., A. Sharaiha, and S. Collardey, "Miniature and superdirective two elements endfire antenna array," *8th European Conference on Antennas and Propagation (EuCAP 2014)*, Apr. 6–11, 2014.
7. Haskou, A. and A. Sharaiha, "Integrating superdirective electrically small antenna arrays in PCBs," *IEEE Antennas and Wireless Propagation Letters*, Jan. 2015.
8. Haskou, A., A. Sharaiha, and S. Collardey, "Design of small parasitic loaded superdirective end-fire antenna arrays," *IEEE Trans. Antennas Propag.*, Vol. 63, No. 12, 5456–5464, Dec. 2015.
9. Harrington, R. F., "A Reactively controlled directive arrays," *IEEE Trans. Antennas Propag.*, Vol. 26, No. 3, 390–395, May 1978.
10. Milne, R., "A small adaptive array antenna for mobile communications," *Antennas and Propagation Society International Symposium*, Vol. 23, 797–800, 1985.
11. Zhang, T., S. Y. Yao, and Y. Wang, "Design of radiation-pattern-reconfigurable antenna with four beams," *IEEE Antennas Wireless Propag. Lett.*, Vol. 14, 183–186, 2015.
12. Dihissou, A., A. Diallo, P. Le Thuc, and R. Staraj, "Directive and reconfigurable loaded antenna array for wireless sensor networks," *Progress In Electromagnetics Research C*, Vol. 84, 103–117, 2018.
13. Jacob, M. M., et al., "Broadband non-Foster matching of an electrically small loop antenna," *IEEE Antennas and Propagation Society International Symposium (APSURSI)*, 2012.